Thiol-functionalization of Mn5Ge3 thin films

Marta K Schütz, Matthieu Petit, Lisa Michez, Alain Ranguis, Guillaume Monier, Christine Robert-Goumet, Jean-Manuel Raimundo

Published in Applied Surface Science, available online 04/30/2018

DOI: 10.1016/j.apsusc.2018.04.231

Article + supplementary informations

Thiol-functionalization of Mn_5Ge_3 thin films

Marta K. Schütz[1+] Matthieu Petit[1*] Lisa Michez[1] Alain Ranguis[1] Guillaume Monier[2] Christine Robert-Goumet[2] Jean-Manuel Raimundo[1*]

[1]Centre Interdisciplinaire de Nanoscience de Marseille (CINaM), Aix Marseille Université, CNRS, CINaM UMR CNRS 7325, 13288 Marseille, France

[2]Institut Pascal, Université Clermont Auvergne, CNRS, SIGMA, F-63000 Clermont-Ferrand, France

Present address:

[+]School of Chemistry, Pontifical Catholic University of Rio Grande do Sul (PUCRS), Av. Ipiranga, 6681, Porto Alegre, RS, Brazil.

[*]Corresponding authors: jean-manuel.raimundo@univ-amu.fr, matthieu.petit@univ-amu.fr

HIGHLIGHTS

The surface state of Mn_5Ge_3 exposed to air and common colvents, is analyzed by XPS.

The surface free energy of Mn_5Ge_3 is calculated with the OWRK method.

The grafting of Mn_5Ge_3 films by octane- and perfluorodecane-thiol SAMs is proposed.

KEYWORDS

thiol; passivation; self-assembled monolayers; manganese germanide; Mn_5Ge_3; wettability; spintronics; surface free energy.

ABSTRACT

Hybrid organic/inorganic interfaces could pave the way to chemically designed or new multifunctional electronic devices, in particular in the spintronics field where, for instance, the interfacial spin polarization can be tuned through chemical interactions and surface modifications. We report herein, for the very first time, the assays of self-assembled monolayers (SAMs) formation on Mn_5Ge_3 surface. Interestingly, Mn_5Ge_3 is a ferromagnetic metal possessing interesting features for spintronics such as a high Curie temperature, a capability to grow epitaxially on Ge germanium that is a key point for integration in the mainstream Si technology. Mn_5Ge_3 thin films are synthesized by molecular beam epitaxy under ultra-vacuum condition. We studied the Mn_5Ge_3 surface prior to deposition of SAMs, meaning the surface exposed to air and different solvents, by XPS and contact angle measurements leading to the value of the surface tension of this surface. Then SAMs of octanethiol and perfluorodecanethiol are formed on Mn_5Ge_3 surface at room temperature. The best experimental conditions to form the SAMs are found for an immersion time of 36 h and a concentration of 4 mM.

1 INTRODUCTION

Over the last decade the manganese germanide Mn_5Ge_3 has appeared to be a potential candidate for spin injection into group-IV semiconductors due to its room-temperature ferromagnetism properties (Curie temperature T_C= 297 K), high spin polarization, metallic character, ability to epitaxially grow on Ge(111) substrates as well as compatibility with the already-existing Si-Ge-based technology [1–3]. Moreover, several studies have shown that its T_C can be enhanced by carbon doping into the interstitial sites of the Mn_5Ge_3 lattice and that the Schottky contact between Ge and Mn_5Ge_3 may be suitable for electrical spin injection [4–7]. Furthermore, hybrid structures of organic molecules and inorganic materials have been recently in the spintronic community's crossroad. The first purpose was to use the molecules as spin transport media because of the rather weak coupling between the spin and orbital momentum of the electron that allows keeping the spin orientation over long distances. It has been rapidly anticipated that molecules could also have strong impacts on the magnetic properties, for instance, several teams dealing with spin valves reported negative magnetoresistance [8,9]. These phenomena confirmed the growing interest on the developing molecular “spinterface” which could lead to single multi-functional devices thanks to the “LEGO” capability of molecular engineering [10–13]. Molecules and biomolecules possessing a magnetic core are potential candidates to be grafted on the magnetic substrate Mn_5Ge_3. One of the most promising approaches to modify surface involves the

deposition of organic self-assembled monolayers (SAMs). SAMs constitute a method of choice to achieve highly dense and ordered thin films, robustly anchored to large surface areas either on clean metallic (e.g. Au, Ag), oxidized (e.g. SiO_2, ITO) or semiconducting (e.g. Si, Ge) substrates. This method does not require either sophisticated and expensive instrumentation, or intricate sample preparations, expert manpower and allows the opportunity to vary both the length of the chains and functional groups to manipulate macroscopic properties of the surface, such as wettability, biocompatibility and protein/cellular adhesion [14–17]. Furthermore, magnetic properties of metals and diluted magnetic semiconductors (DMS) such as (Ga, Mn)As have been tailored by SAMs surface modifications leading to induced magnetic moments or modification of ferromagnetic properties [18–20].

Alkanethiols are so far the most studied self-assembled molecules because of the covalent polarized bond formed between thiol headgroups and appropriate substrates (e.g. Au, Ge, Ag, Cu, Pt, Hg, GaAs). Regarding Ge surface, HBr and HCl are often used to halogenate the surface of this semiconductor prior to the SAMs formation, mainly to avoid the process of reoxidation of the surface. Indeed, the classical hydrogenation, which is used for silicon surface passivation, is less stable in the case of the Ge surface [21–25]. The inherent ability of adsorbed monolayers to modify physicochemical properties of surfaces makes this approach attractive to implement the organic functionalization of the surface of the Mn_5Ge_3/Ge system. To the best of our knowledge, functionalization of Mn_5Ge_3/Ge with alkylthiols has never been done before. The Mn_5Ge_3 thin films being elaborated under ultra high vacuum conditions by molecular beam epitaxy (MBE), we present herein a study of the surface state of the Mn_5Ge_3 thin films under air and common solvents exposure and secondly the first insights on the functionalization of Mn_5Ge_3 with thiol molecules.

2 MATERIALS AND METHODS

2.1 Substrates.

Sb-doped Ge(111) wafers (n-type, 600 µm thickness, 12-16 Ω cm) were purchased from Umicore (Belgium). Mn_5Ge_3/Ge(111) heterostructures were grown by molecular beam epitaxy (MBE) technique according to the method described by Petit *& al* [26]. This method is based on the co-deposition at room temperature of Mn and Ge. It allows growing high crystalline quality films of Mn_5Ge_3 with an

abrupt interface on Ge(111) and with a small RMS roughness (ca. 2 nm). The Mn_5Ge_3 thin films were 30 nm thick.

2.2 Grafting procedures.

2.2.1 Cleaning. Mn_5Ge_3/Ge(111) substrates were first successively sonicated in acetone, deionized water and ethanol. Each cleaning step was repeated three times with a fresh solvent for 5 min, followed by blow-drying with argon gas.

2.2.2 Thiol-functionalization. Cleaned Mn_5Ge_3/Ge(111) substrates were immersed into octanethiol (OT) ($CH_3(CH_2)_7SH$, Alfa Aesar) or perfluorodecanethiol (PFDT) ($CF_3(CF_2)_7CH_2CH_2SH$, Sigma-Aldrich) solutions for surface functionalization. The experiments were carried out at room temperature to avoid any interdiffusion of Ge and Mn at the Mn_5Ge_3/Ge interface that could be detrimental for further spintronic applications. Freshly thiol solutions were prepared in ethanol prior to be used. The vials were backfilled with argon gas in order to minimize O_2 in the headspace. After experiments, the substrates were rinsed three times with ethanol to remove physisorbed molecules on the surface and dried over 24 h in a desiccator at room temperature. We have mainly investigated two parameters: i) the thiol concentration (from 1 to 5 mM) and ii) the immersion reaction time (from 12 to 24, 36, 48 and 72 h). First, a range of concentration of thiol was tested, at fixed immersion time of 24h, in order to determine the optimal concentration needed. Optimum condition of concentration was selected (4 mM, see the Results and Discussion) and experiments were conducted by varying the immersion times.

2.3 Characterizations.

Foremost, a chemical analysis of the untreated Mn_5Ge_3 substrates have been done by X-ray photoelectrons spectroscopy (XPS) in an ultrahigh vacuum system equipped with an Omicron DAR 400 X-ray source. The Mg anode was used to perform the analysis. The hemispherical analyser (HSA) is an Omicron EA 125 (normal detection was used). The angle between the X-ray source and the HSA was equal to 55°. The topographies of the substrates were imaged by atomic force microscopy (AFM) with a Nanoscope IIIA Multimode (Digital instruments) equipped with a 10×10×2.5 µm scanner. The images were recorded in the tapping mode at room temperature using silicon nitride probes (HQ: NSC15/AL BS, Mikromasch). The curvature radius of the silicon tips was about 8 nm (from the supplier specifications). Contact angle measurements were performed for the assessment of the hydrophobic-hydrophilic character of the substrates. Static contact angles (CA) were measured with an OCA 15 apparatus (DataPhysics) at room temperature using the sessile drop method and image

analysis of the drop profile (SCA20 software). Deionized water droplet volume was 5 µL, and the contact angle was measured 10 s after the drop was deposited onto the surface.

3 RESULTS AND DISCUSSION

3.1 Characterization of the Mn_5Ge_3/Ge(111) substrates before the grafting process.

3.1.1 XPS: The Mn_5Ge_3 samples were grown in a MBE chamber and taken out from the UHV chamber for the grafting process. The different samples were exposed successively to atmosphere and chemical cleaning prior undergoing the SAMs grafting procedures. To our knowledge this is the first report describing both aging changes of the Mn_5Ge_3 surface under air exposure, stability under chemical cleaning/etching with polar aprotic or protic solvents such as acetone and ethanol respectively.

After air exposure, Mn_5Ge_3 surface has been analyzed by XPS in order to determine the chemical state of the surface atoms and then the surface free energy has been measured. The Ge_{3d}, O_{1s} and Mn_{2p} core levels were recorded and the parameters for the XPS fits are given in the electronic supplementary information (ESI). The Figure 1 shows the electronic state of the Mn_5Ge_3 surface after air exposure. Figures 1a and 1b exhibit the evolution of the Ge_{3d} core level before (cleaned) and after air exposure whereas fig. 1c concerns the evolution of the Mn_{2p} core level. The “cleaned” Ge_{3d} core level exhibits one peak at 29.1 eV, related to Ge atoms in the bulk state in Mn_5Ge_3 (blue contributions in Figure 1a and 1b respectively). On Fig.1b, the peak around 31.5 eV is typical of germanium oxide. It can be deconvoluted into two main contributions corresponding to the Ge atoms in the oxidized states Ge^{2+} and Ge^{3+} [27]. Thus, the oxidized state of the Ge atoms differs from a cleaned (non oxidized) Mn_5Ge_3 surface and to a Ge(111) substrate in which the Ge^{4+} state, corresponding to the GeO_2 oxide (see ESI), is prevailing. This difference is also confirmed by the analysis of the O_{1s} core levels (see ESI). Regarding the Mn_{2p} core level (Fig. 1c), the oxidation by air leads to a strong shift of about 2.5 eV at higher energy that could be attributed to the Mn atoms in oxidized states around $2\text{-}2.7^{+}$ similar to those found in MnO or Mn_3O_4 [28]. These features confirm a clear difference for the native oxide structures of Ge(111) and Mn_5Ge_3 suggesting that the latter may correspond to a ternary oxide of Mn-Ge-O.

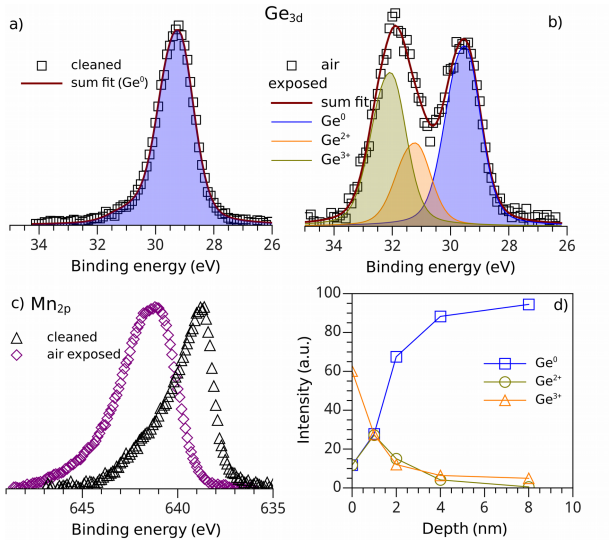

Figure 1: XPS spectra related to the effect of air exposure on the Mn_5Ge_3 surfaces. a) Reference: Ge_{3d} core level of a cleaned (non oxidized) Ge(111) substrate. b) Deconvolution of the Ge_{3d} core levels from an oxidized Mn_5Ge_3 surfaces. c) Superposition of $Mn_{2p3/2}$ core levels of a cleaned and oxidized Mn_5Ge_3 layers. d) Evolution of the contributions of the Ge_{3d} core level according to a depth profile of oxidized Mn_5Ge_3 thin films done by ionic Ar^+ bombardment.

Moreover the Fig. 1d exhibits the evolution of the Ge^0 as well as the oxide contributions Ge^{2+} and Ge^{3+} for the Ge_{3d} core level along a depth profile in the oxidized Mn_5Ge_3 layer. The depth profile has been made using an Ar^+ ionic sputtering. We have evidenced that the oxidation of the Mn_5Ge_3 thin film took place in the first 4 nm, after one week of air exposure. This indicates that the oxidation of the Mn_5Ge_3 film is not limited to the very surface and oxygen diffuses into the layer. Prior the SAMs formation, the Mn_5Ge_3 film surface is successively cleaned with acetone then ethanol and carefully analysed each step by XPS (Figure 2). The Ge3d core level is followed after each solvent rinse highlighting specific behaviours (Fig. 2a, 2b). For instance, after acetone cleaning, the surface exhibits a Ge^{4+} contribution unlike the ethanol case. The deconvolution profile after ethanol treatment is very similar to the one of the air exposed sample and also the intensity of the overall oxide component is smaller than in that

case. This last observation could be explained by the fact that GeO_2 is soluble in water and that we used a 96% ethanol. This is consistent with several studies regarding the influence of wet surface treatments and SAM deposition processes which have demonstrated that water or a mixture of water and ethanol can dissolve germanium oxide [24,29,30]. Surprisingly, concerning the $Mn_{2p3/2}$ and O_{1s} core levels (Fig. 2c and 2d), no significant discrepancy can be noticed. The O_{1s} shapes slightly differ due to the stoichiometry changes of the oxide accordingly to the solvent used and to the water sensitivity of the germanium oxide component of the overall oxide.

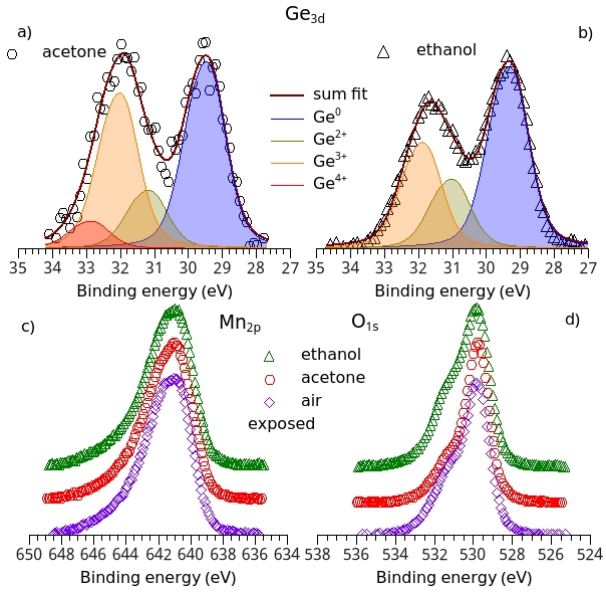

Figure 2: XPS analysis of the Mn_5Ge_3 surface after exposure to acetone and ethanol. a) and b) Ge_{3d} core level. c) $Mn_{2p3/2}$ and d) O_{1s} core levels. (For c) and d), the air exposed case is included as a comparison).

These XPS results clearly show that the oxide layer does not consist only on a germanium oxide layer but contains also a manganide part. Consequently the nature of the oxide layer may be close to that of a ternary oxide Mn-O-Ge. The oxidation state of the Mn_5Ge_3 oxide layer slightly changes depending on environmental conditions. This observation was also carried out on Ge surfaces, which are known to exhibit Ge^{2+} and/or Ge^{4+} oxidation states depending on the surface treatments [31,32].

3.1.2 Surface free energy (SFE): SFE determinations have been achieved using the Owens, Wendt, Rabel and Kaelble (OWRK) method with the measure of the contact angles (CAs), with different liquids (deionized water, formamide, glycerol and dichloromethane), on the air exposed Mn_5Ge_3

surface [33–35]. Based on the Fowkes' method, the surface free energy is divided into a polar part (non-dispersive, P) and a dispersive part (D) (Eq.1) [36]:

$$\sigma_{sl} = \sigma_s + \sigma_l - 2\left(\sqrt{\left(\sigma_s^D \sigma_l^D\right)} + \sqrt{\left(\sigma_s^P \sigma_l^P\right)}\right) \quad \text{(Eq.1)}$$

The interfacial tension σ_{sl} between liquid and solid is calculated with the two surface tensions σ_s and σ_l of the solid and the liquid and the similar interactions between the phases. These interactions are interpreted as the geometric mean of a dispersive component σ^D and a polar one σ^P of the surface tension. The Figure 3 displays the plot of the OWRK method.

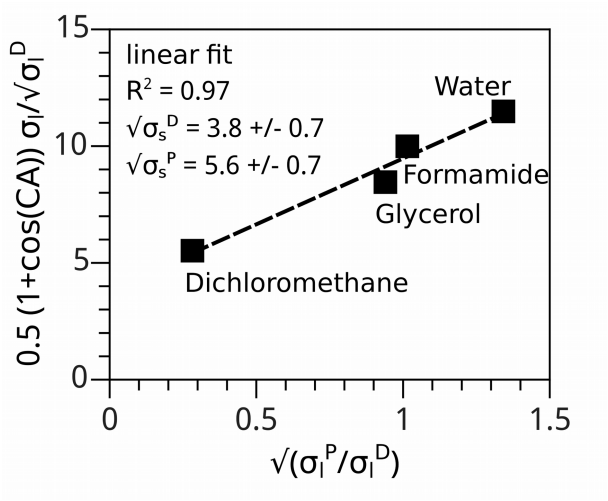

Figure 3: Plot of the Owens, Wendt, Rabel and Kaelble method for calculating the surface free energy of the Mn_5Ge_3 thin film exposed to air.

The corresponding linear fit affords a dispersive contribution of σ^D_{Mn5Ge3} = 14.7 mJ.m^{-2} and a polar part of σ^P_{Mn5Ge3} = 31.8 mJ.m^{-2}, which corresponds to a total SFE of σ_{Mn5Ge3} = 46.5 mJ.m^{-2}. As for comparison, the SFE of SiO_2, an extensively studied surface for SAM deposition, is within the range of 40-77 mJ.m^{-2} with a predominance of the polar component fostering the interactions with polar head-groups such as thiol derivatives [37–39]. In addition, it is known that under vacuum conditions, the surface of Mn_5Ge_3 is terminated by Mn atoms therefore the SFE value of an unchanged surface might be close to that of the Mn metal, around 1350-1600 mJ.m^{-2} [40,41]. Moreover, the reported SFE value for a pure manganese oxide surface (Mn_3O_4, 72 mJ.m^{-2}) supports the XPS data, evidencing that the surface of a Mn_5Ge_3 thin film is strongly affected both by air exposition and solvents treatments [42].

3.2 Grafting of the Mn_5Ge_3/Ge(111) substrates.

The Mn_5Ge_3/Ge(111) substrates have been subjected to SAMs surface modifications with two different alkyl thiols namely OT and PFDT (1-octanethiol and perfluorodecanethiol, respectively) by varying the thiol concentrations and then the immersion reaction times. The morphology and wettability of the newly formed SAMs were investigated with AFM and water CA measurements, respectively, for a given immersion time of 24h. The surfaces roughness obtained from the AFM images and the CA values are presented on the Figures 4a and 4b (the AFM images are available in the ESI).

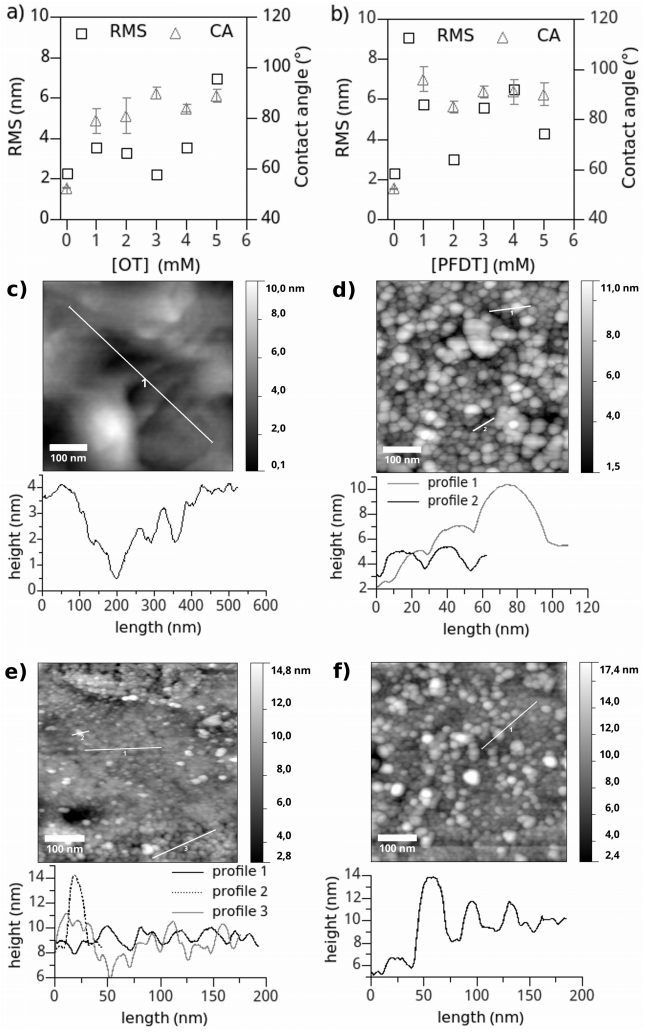

Figure 4: a)-b) RMS Roughness (from 2×2 μm^2 AFM images) and water CA versus thiol molecule concentrations for Mn_5Ge_3 surfaces grafted with a) OT and b) PFDT SAMs. (Immersion time = 24h). c)-f) AFM images 500×500nm^2 of OT SAMs for concentration of 0 (image c) (i.e. Mn_5Ge_3 bare

surface), 3 (image d), 4 (image e) to 5 mM (image f) respectively, along with the corresponding profile cross-sections.

It was observed that OT molecules could easily chemisorb onto the Mn_5Ge_3 surface without any significant changes in the surface roughness, except for concentrations ≥ 5 mM. Increasing the solutions concentration (≥ 5 mM) ensue the formation of multilayers that affect dramatically the roughness (fig. 4f). Noteworthy, if the concentration is lower than 4 mM (Figures 4d: 3mM, 4e: 4mM) small separated aggregates of about 30-50 nm in diameter and 2-2,5 nm in height are present within the monolayer. This height is in the range of the length of the grafted molecules (~2,5 nm). A different behaviour was obtained when PFDT was used to passivate the surface of the substrate. Results obtained with PFDT molecules exhibited higher RMS roughness on average but with a greater dispersion of the values. Water CA measurements for each experiment have revealed that the hydrophobicity of the Mn_5Ge_3/Ge SAM-modified substrate does not significantly change between both thiol molecules regardless the used concentration for an immersion reaction time of 24 hours, reaching values around 85°. However, PFDT molecules provided the highest values of CA at lower concentrations than OT grafting which is normally expected due to higher hydrophobic character of the perfluoroalkyl chains compared to the alkyl chains.

In order to evaluate the effect of the immersion time on the Mn_5Ge_3/Ge functionalization, we have performed the experiments with OT solutions at a concentration of [C] = 4 mM as, both the dispersion of the RMS roughness and the CA values are lower than those measured with the PFDT. The immersion reaction time was varied from 12 to 72 hours. RMS roughness and the water CA are displayed in Figure 5.

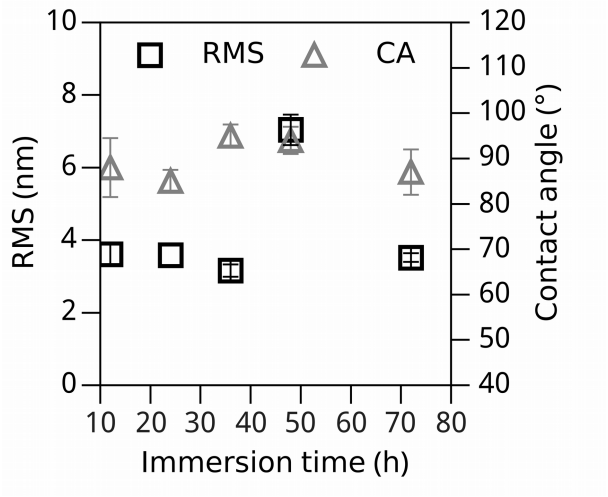

Figure 5: RMS roughness and water CA of Mn_5Ge_3/Ge substrates after functionalization with 4 mM OT as a function of immersion time.

No significant difference on the hydrophobicity nor the roughness of the surface was observed by varying the immersion time. The maximum value of the CA was obtained for 36h of immersion and reached 95°, before decreasing slightly. However, the grafting process occurs before 12h of immersion. We observed by AFM (not shown here) that a more homogeneously ordered and dense layer is formed after 36 hours of immersion whereas prolonged immersion time (> 48 hours) conducts to the formation of aggregates and less ordered layers. This behaviour is similar to the kinetic observed for n-alkylthiolates in 1:1 water-ethanol solvents mixture deposited on Ge surfaces [21,24]. Nevertheless, the measured CAs remain lower than the ones reported on Ge surfaces, around 100-110°. This feature could be ascribed to an uncompleted coverage of the Mn_5Ge_3 surface by the OT SAM or a deterioration of the SAM upon extended immersion time that could facilitate the diffusion of ethanol till the film surface and leading to a possible dissolution of the oxide layer (attested by a decrease of the CA after 36h).

4 CONCLUSIONS

We presented herein a simple and effective method to deposit SAMs on Mn_5Ge_3 thin films. We have evidenced that thiol derivatives (i.e. OT and PFDT) can easily chemisorb onto Mn_5Ge_3 surface as self-assembled monolayers. Our results showed that changes in surface roughness are more pronounced with PFDT than with OT molecules. The optimal conditions, based on the concentrations and immersion reaction time, to ensure well-ordered, dense and homogeneous SAMs were found to be a thiol concentration of [C] = 4 mM and an immersion time of 36 hours. Higher values of these parameters resulted mainly in an increase of the surface roughness due to the formation of aggregates on the surface and less ordered SAM layers. Comparing the SAMs from OT and PFDT we did not observe any significant changes in the wettability properties of the film surface even it was expected that perfluorinated alkylthiols could render the Mn_5Ge_3 surfaces more hydrophobic (C–F bonds are more hydrophobic than the C–H bonds). Further improvements on the deposition methodologies still need to be matured for Mn_5Ge_3 substrate and could lean for instance towards the use of a solvent

mixture of 1:1 ethanol-water and a process temperature around 60-80°C which has been proved to be efficient for the deposition of SAMs onto Ge substrates [21,24]. Moreover, further XPS analysis should be performed on the grafted surfaces so as to assess the formation of the covalent polarized bonds between the molecules and the Mn_5Ge_3 substrate. Nevertheless this seminal report on functionalization of Mn_5Ge_3 paves the way to new routes and new opportunities for modifications to access to novel hybrid materials in combination with the fascinating magnetic properties of Mn_5Ge_3.

ACKNOWLEDGEMENT

M.K.S. acknowledges the National Council of Scientific and Technologic Development (CNPq) of the Brazilian Ministry of Science, Technology and Innovation (MCTI) for the postdoctoral fellowship. All the authors are thankful to C Gérard from the Chemical-biochemical service of the CINaM, for the surface free energy measurements.

REFERENCES

[1] C. Zeng, S.C. Erwin, L.C. Feldman, A.P. Li, R. Jin, Y. Song, et al., Epitaxial ferromagnetic Mn5Ge3 on Ge(111), Appl. Phys. Lett. 83 (2003) 5002–5004. doi:10.1063/1.1633684.

[2] V. Le Thanh, A. Spiesser, M.-T. Dau, S. F Olive-Mendez, L. A Michez, M. Petit, Epitaxial growth and magnetic properties of Mn5Ge3/Ge and Mn5Ge3Cx/Ge heterostructures for spintronic applications, Adv. Nat. Sci. Nanosci. Nanotechnol. 4 (2013) 43002. doi:10.1088/2043-6262/4/4/043002.

[3] S.F. Olive-Mendez, A. Spiesser, L.A. Michez, V. Le Thanh, A. Glachant, J. Derrien, et al., Epitaxial growth of Mn5Ge3/Ge(111) heterostructures for spin injection, Thin Solid Films. 517 (2008) 191–196. doi:DOI: 10.1016/j.tsf.2008.08.090.

[4] M. Gajdzik, C. Sürgers, M.T. Kelemen, H. v. Löhneysen, Strongly enhanced Curie temperature in carbon-doped Mn5Ge3 films, J. Magn. Magn. Mater. 221 (2000) 248–254. doi:DOI: 10.1016/S0304-8853(00)00494-7.

[5] I. Slipukhina, E. Arras, P. Mavropoulos, P. Pochet, Simulation of the enhanced Curie temperature in Mn5Ge3Cx compounds, Appl. Phys. Lett. 94 (2009) 192505. doi:10.1063/1.3134482.

[6] A. Spiesser, I. Slipukhina, E. Arras, V. Le Thanh, L. Michez, P. Pochet, et al., Control of magnetic properties of epitaxial Mn5Ge3Cx films induced by carbon doping, Phys. Rev. B. 165203 (2011) 1–7. doi:10.1103/PhysRevB.84.165203.

[7] M. Petit, R. Hayakawa, Y. Wakayama, V. Le Thanh, L. Michez, V. Le Thanh, et al., Mn5Ge3C0.6 /Ge(111) Schottky contacts tuned by an n-type ultra-shallow doping layer, J. Phys. D. Appl. Phys. 49 (2016) 355101. doi:10.1088/0022-3727/49/35/355101.

[8] S. Ding, Y. Tian, Y. Li, W. Mi, H. Dong, X. Zhang, et al., Inverse Magnetoresistance in Polymer Spin Valves, ACS Appl. Mater. Interfaces. 9 (2017) 15644–15651. doi:10.1021/acsami.7b02804.

[9] W. Xu, G.J. Szulczewski, P. Leclair, I. Navarrete, R. Schad, G. Miao, et al., Tunneling magnetoresistance observed in La0.67 Sr0.33 Mn O3 /organic molecule/Co junctions, Appl. Phys. Lett. 90 (2007) 9–11. doi:10.1063/1.2435907.

[10] M. Galbiati, S. Tatay, A. V Dediu, R. Mattana, P. Seneor, Spinterface: Crafting spintronics at the molecular scale, MRS Bull. 39 (2014) 602–607. doi:10.1557/mrs.2014.131.

[11] M. Cinchetti, V.A. Dediu, L.E. Hueso, Activating the molecular spinterface, Nat. Mater. 16 (2017) 507–515. doi:10.1038/nmat4902.

[12] J.S. Moodera, B. Koopmans, P.M. Oppeneer, On the path toward organic spintronics, MRS Bull. 39 (2014) 578–581. doi:10.1557/mrs.2014.128.

[13] T.L.A. Tran, D. Çakir, P.K.J. Wong, A.B. Preobrajenski, G. Brocks, W.G. Van Der Wiel, et al., Magnetic properties of bcc-Fe(001)/C60 interfaces for organic spintronics, ACS Appl. Mater. Interfaces. 5 (2013) 837–841. doi:10.1021/am3024367.

[14] A. Ulman, Formation and Structure of Self-Assembled Monolayers, Chem. Rev. 96 (1996) 1533–1554. doi:10.1021/cr9502357.

[15] F. Schreiber, Structure and growth of self-assembling monolayers, Prog. Surf. Sci. 65 (2000) 151–256. doi:10.1016/S0079-6816(00)00024-1.

[16] J.C. Love, L.A. Estroff, J.K. Kriebel, R.G. Nuzzo, G.M. Whitesides, Self-Assembled Monolayers of Thiolates on Metals as a Form of Nanotechnology, Chem. Rev. 105 (2005) 1103–1169. doi:10.1021/cr0300789.

[17] G.M. Whitesides, J.K. Kriebel, J.C. Love, Molecular engineering of surfaces using self-assembled monolayers, Sci. Prog. 88 (2005) 17–48.

[18] X. Wang, H. Wang, D. Pan, T. Keiper, L. Li, X. Yu, et al., Robust Manipulation of Magnetism in Dilute Magnetic Semiconductor (Ga,Mn)As by Organic Molecules, Adv. Mater. 27 (2015) 8043–8050. doi:10.1002/adma.201503547.

[19] T.C. Kreutz, E.G. Gwinn, R. Artzi, R. Naaman, H. Pizem, C.N. Sukenik, Modification of ferromagnetism in semiconductors by molecular monolayers, Appl. Phys. Lett. 83 (2003) 4211–4213. doi:10.1063/1.1625422.

[20] K. V Raman, A.M. Kamerbeek, A. Mukherjee, N. Atodiresei, K. Tamal, V. Caciuc, et al., Interface-engineered templates for molecular spin memory devices, Nature. 493 (2013) 509–513. doi:10.1038/nature11719.

[21] Q. Cai, B. Xu, L. Ye, Z. Di, S. Huang, X. Du, et al., 1-Dodecanethiol based highly stable self-Assembled monolayers for germanium passivation, Appl. Surf. Sci. 353 (2015) 890–901. doi:10.1016/j.apsusc.2015.06.174.

[22] P. Ardalan, C.B. Musgrave, S.F. Bent, Formation of Alkanethiolate Self-Assembled Monolayers at Halide-Terminated Ge Surfaces, Langmuir. 25 (2009) 2013–2025. doi:10.1021/la803468e.

[23] P. Ardalan, Y. Sun, P. Pianetta, C.B. Musgrave, S.F. Bent, Reaction mechanism, bonding, and thermal stability of 1-alkanethiols self-assembled on halogenated Ge surfaces, Langmuir. 26 (2010) 8419–8429. doi:10.1021/la904864c.

[24] J.N. Hohman, M. Kim, H.R. Bednar, J. a. Lawrence, P.D. McClanahan, P.S. Weiss, Simple, robust molecular self-assembly on germanium, Chem. Sci. 2 (2011) 1334. doi:10.1039/c1sc00115a.

[25] X. Lefevre, O. Segut, P. Jegou, S. Palacin, B. Jousselme, Towards organic film passivation of germanium wafers using diazonium salts: Mechanism and ambient stability, Chem. Sci. 3 (2012) 1662–1671. doi:10.1039/c2sc01034h.

[26] M. Petit, L. Michez, C.-E. Dutoit, S. Bertaina, V.O. Dolocan, V. Heresanu, et al., Very low-temperature epitaxial growth of Mn5Ge3 and Mn5Ge3C0.2 films on Ge(111) using molecular beam epitaxy, Thin Solid Films. 589 (2015) 427–432. doi:10.1016/j.tsf.2015.05.068.

[27] D. Schmeisser, R.D. Schnell, A. Bogen, F.J. Himpsel, D. Rieger, G. Landgren, et al., Surface oxidation states of germanium, Surf. Sci. 172 (1986) 455–465. doi:10.1016/0039-6028(86)90767-3.

[28] J.C. Carver, G.K. Schweitzer, T.A. Carlson, Use of XRay Photoelectron Spectroscopy to Study Bonding in Cr, Mn, Fe, and Co Compounds, J. Chem. Phys. 57 (1972) 973. doi:10.1063/1.1678348.

[29] B. Onsia, T. Conard, S. De Gendt, M. Heyns, I. Hoflijk, P. Mertens, et al., A study of the influence of typical wet chemical treatments on the germanium wafer surface, Diffus. Defect Data. Solid State Data. Part B, Solid State Phenom. 103–4 (2005) 27–30. http://www.refdoc.fr/Detailnotice?idarticle=7022063.

[30] K. Prabhakaran, T. Ogino, Oxidation of Ge(100) and Ge(111) surfaces: an UPS and XPS study, Surf. Sci. 325 (1995) 263–271. doi:10.1016/0039-6028(94)00746-2.

[31] T. Hanrath, B.A. Korgel, Chemical Surface Passivation of Ge Nanowires, J. Am. Chem. Soc. 126 (2004) 15466–15472. doi:10.1021/ja0465808.

[32] G. Collins, J.D. Holmes, Chemical functionalisation of silicon and germanium nanowires, J. Mater. Chem. 21 (2011) 11052. doi:10.1039/c1jm11028d.

[33] W. Rabel, Einige Aspekte der Benetzungstheorie und ihre Anwendung auf die Untersuchung und Veränderung der Oberflächeneigenschaften von Polymeren, Farbe Und Lack. 77 (1971) 997–1005.

[34] D.K. Owens, R.C. Wendt, Estimation of the surface free energy of polymers, J. Appl. Polym. Sci. 13 (1969) 1741–1747. doi:10.1002/app.1969.070130815.

[35] D.H. Kaelble, Dispersion-Polar Surface Tension Properties of Organic Solids, J. Adhes. 2 (1970) 66–81. doi:10.1080/0021846708544582.

[36] F.M. Fowkes, Attractives forces at interfaces, Ind. Enginnering Chem. 56 (1964) 40–52. doi:10.1021/ie50660a008.

[37] E.J. Chibowski, Surface free energy and wettability of silyl layers on silicon determined from contact angle hysteresis, Adv. Colloid Interface Sci. 113 (2005) 121–131. doi:10.1016/j.cis.2005.01.005.

[38] F. Hejda, P. Solar, J. Kousal, Surface Free Energy Determination by Contact Angle Measurements – A Comparison of Various Approaches, WDS'10 Proc. Contrib. Pap. (2010) 25–30.

[39] P. Miskiewicz, S. Kotarba, J. Jung, T. Marszalek, M. Mas-Torrent, E. Gomar-Nadal, et al., Influence of SiO2 surface energy on the performance of organic field effect transistors based on highly oriented, zone-cast layers of a tetrathiafulvalene derivative, J. Appl. Phys. 104 (2008) 1–5. doi:10.1063/1.2968441.

[40] M.-T. Dau, V. Le Thanh, L. a Michez, M. Petit, T.-G. Le, O. Abbes, et al., An unusual phenomenon of surface reaction observed during Ge overgrowth on Mn5Ge3/Ge(111) heterostructures, New J. Phys. 14 (2012) 103020. doi:10.1088/1367-2630/14/10/103020.

[41] F. Aqra, A. Ayyad, Surface energies of metals in both liquid and solid states, Appl. Surf. Sci. 257 (2011) 6372–6379. doi:10.1016/j.apsusc.2011.01.123.

[42] S. Kulkarni, D. Puthusseri, S. Thakur, A. Banpurkar, S. Patil, Hausmannite Manganese oxide cathodes for supercapacitors: Surface Wettability and Electrochemical Properties, Electrochim. Acta. 231 (2017) 460–467. doi:10.1016/j.electacta.2017.01.165.

Electronic Supplementary Informations (ESI)

Thiol-functionalization of Mn_5Ge_3 thin films

Marta K. Schütz,[1] Matthieu Petit,[1] Lisa Michez,[1] Alain Ranguis,[1] Guillaume Monier,[2] Christine Robert-Goumet,[2] Jean-Manuel Raimundo[1]**

[1]Centre Interdisciplinaire de Nanoscience de Marseille (CINaM), Aix Marseille Université, CNRS, CINaM UMR CNRS 7325, 13288 Marseille, France

[2]Clermont Université, Université Blaise Pascal, Institut Pascal, BP 10448, F-63000, Clermont-Fd, France

* Corresponding authors: jean-manuel.raimundo@univ-amu.fr, matthieu.petit@univ-amu.fr

1- XPS: Survey spectrum of the Mn_5Ge_3 surface after air exposure

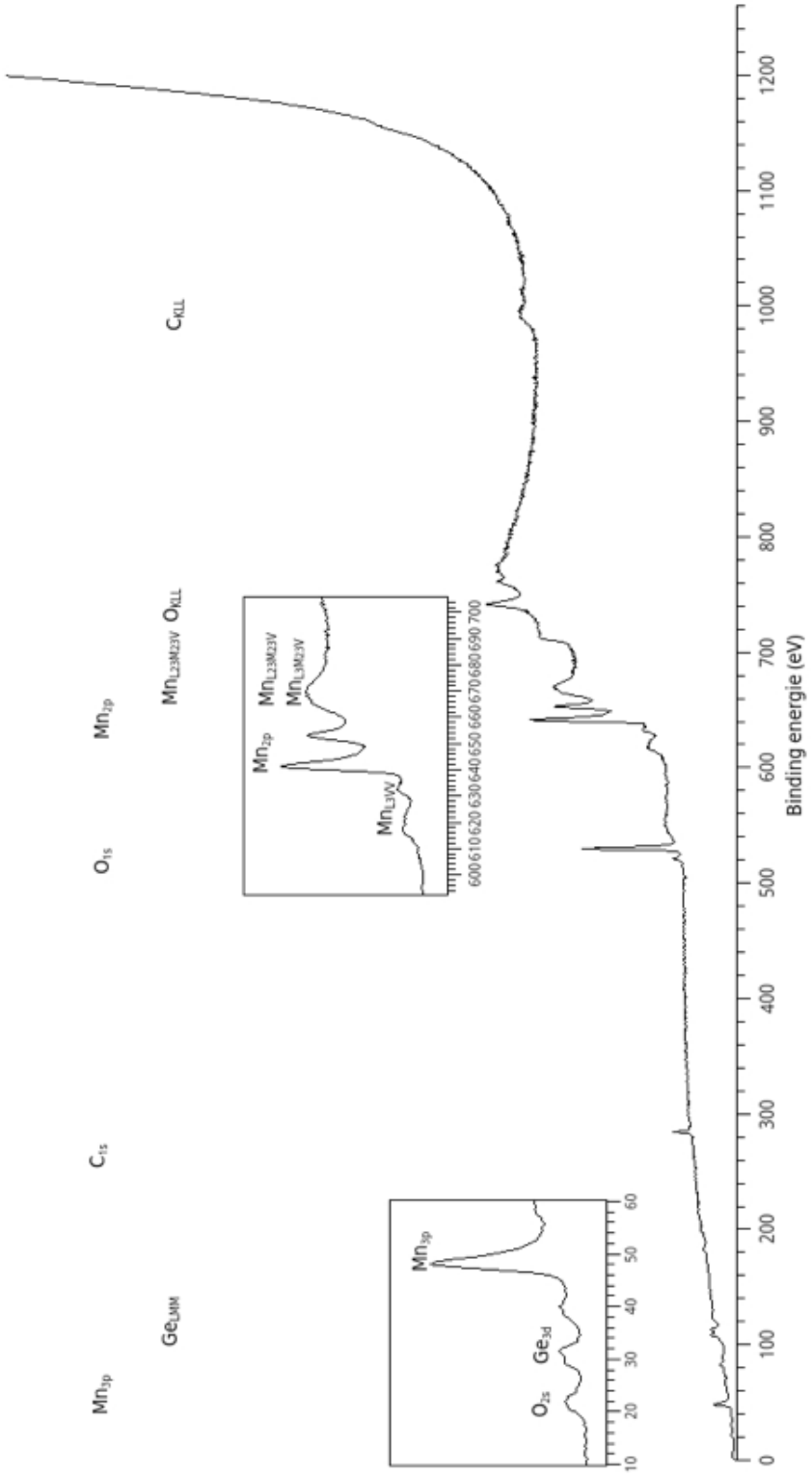

2- Table related to the fitting parameters used to deconvolute the O_{1s} and Ge_{3d} core levels (data in eV: accuracy = +/- 1 eV):

	After air exposure		After chemical rinsing	
	O_{1s}	Ge_{3d}	O_{1s}	Ge_{3d}
FWHM (eV)	1.5	1.1	1.5	1.1
%LG	20	36	20	36
Position of contribution 1 (eV)	529.8	29.1	529.6	29.1
A_1/A_{peak}	0.67	0.43	0.65	0.51
Position of contribution 2 (eV)	531.0	30.9	531.1	30.8
A_2/A_{peak}	0.25	0.20	0.30	0.19
Position of contribution 2 (eV)	532.1	31.7	532.3	31.7
A_3/A_{peak}	0.07	0.37	0.05	0.30

3- Ge_{3d} core levels recorded on (top) a cleaned Ge(111) substrate cleaned Mn_5Ge_3 thin film and (bottom) an oxidized Ge(111) substrate after air exposure. The Ge^{4+} contribution related to the GeO_2 oxide, is prominent

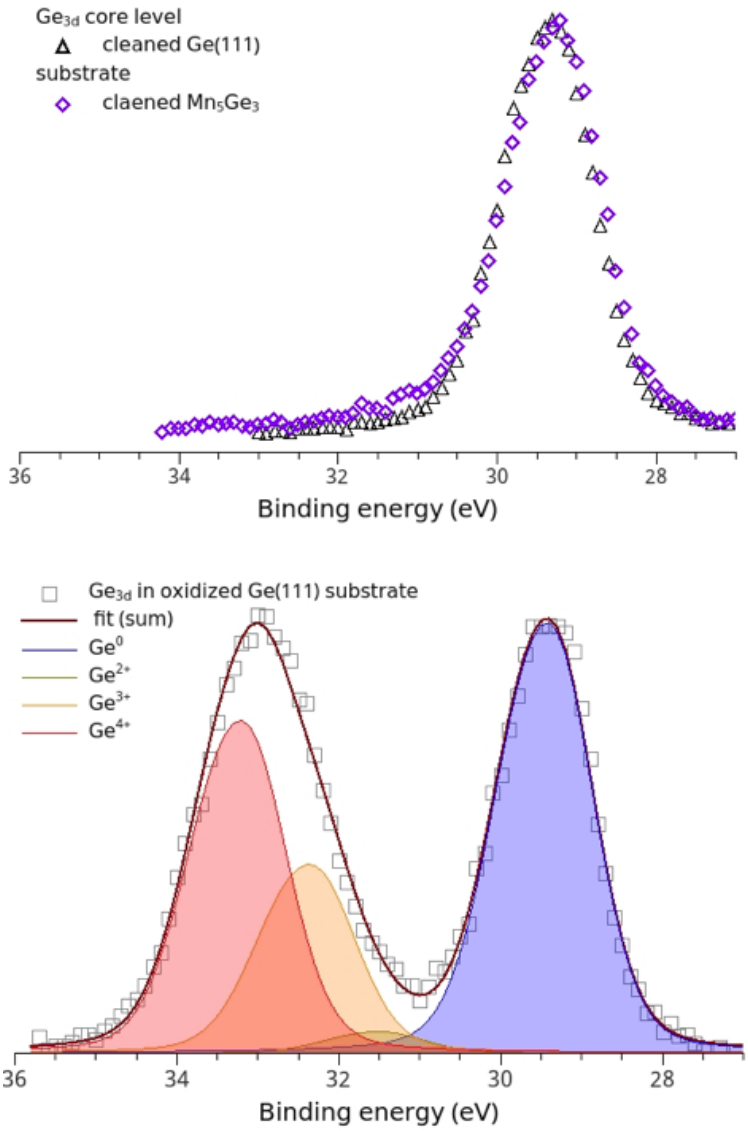

50

55

4- Comparison of the O_{1s} core levels of an oxidized Ge(111) substrate and an oxidized Mn_5Ge_3 thin film after air exposure.

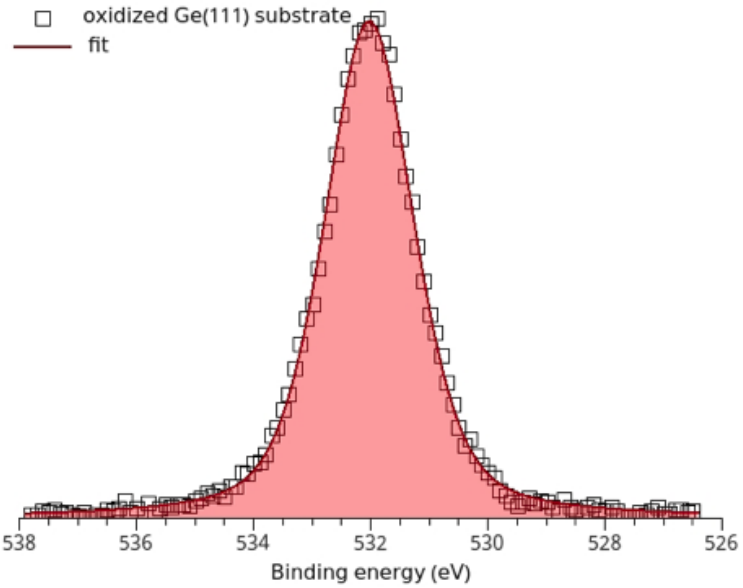

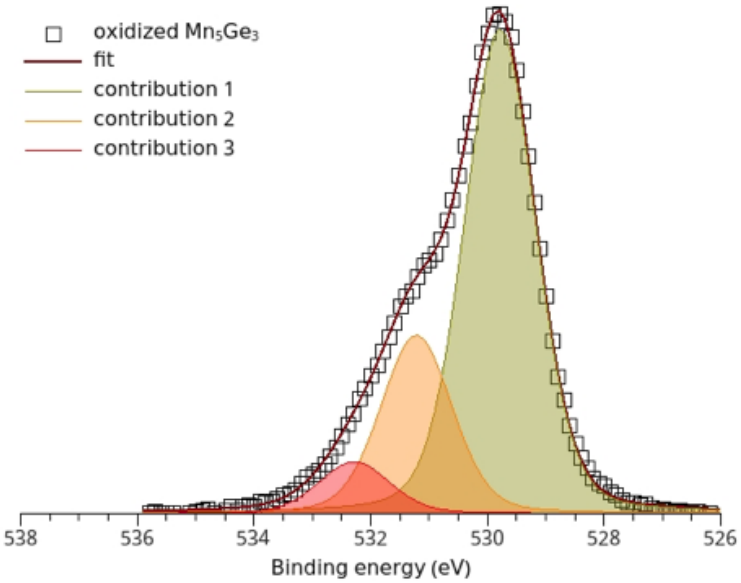

5- 2x2 μm^2 AFM topography images of Mn_5Ge_3/Ge substrate after functionalization with octanethiol (OT) for 24 hours as a function of thiol concentration: a) Mn_5Ge_3 surface prior to grafting, b)-f) OT concentrations 1, 2, 3, 4, 5 mM.

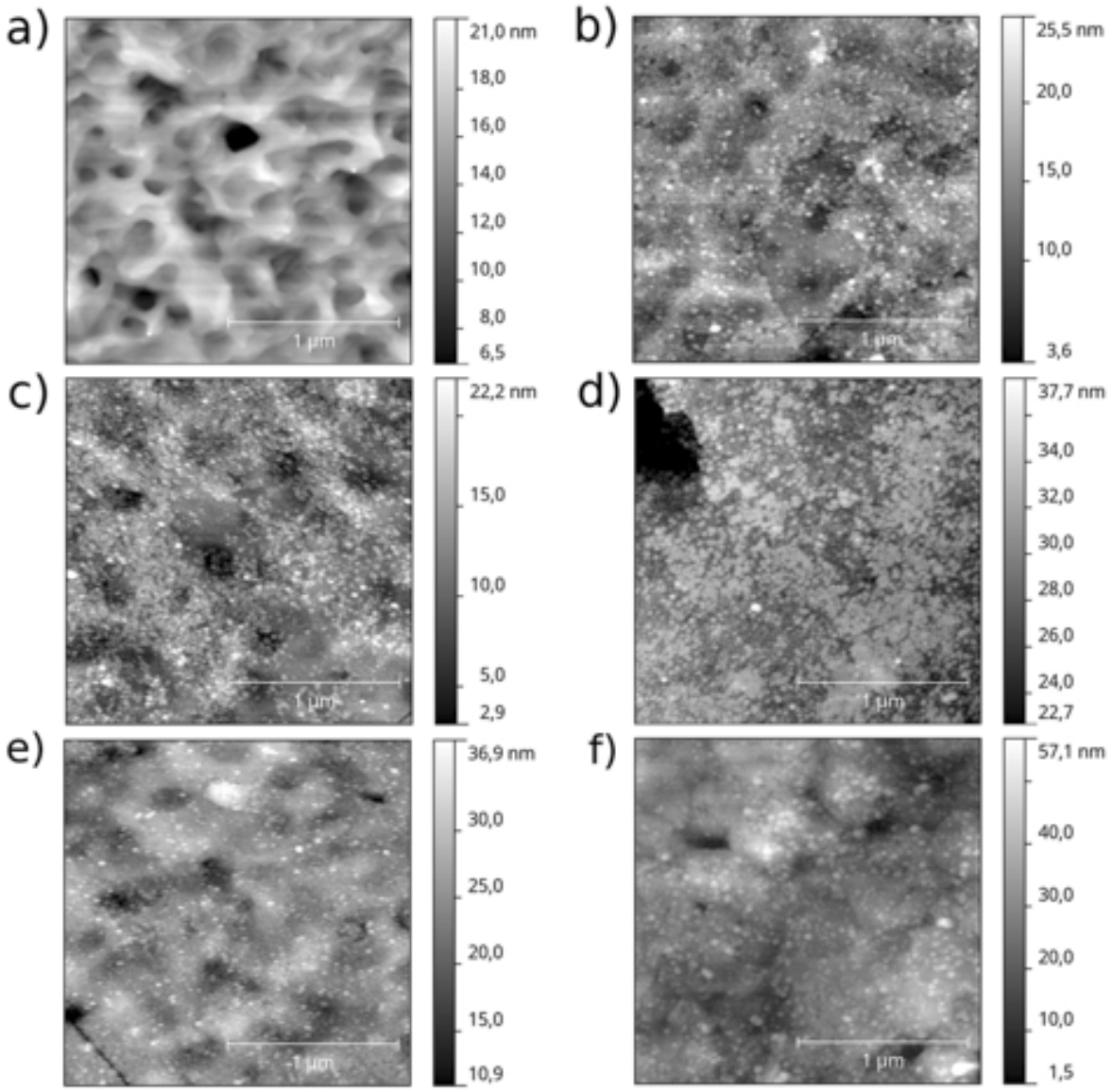

6- 2x2 μm^2 AFM topography images of Mn_5Ge_3/Ge substrate after functionalization with perfluorodecanethiol (PFDT) for 24 hours as a function of thiol concentration: a)-e) PFDT concentrations 1, 2, 3, 4, 5 mM.

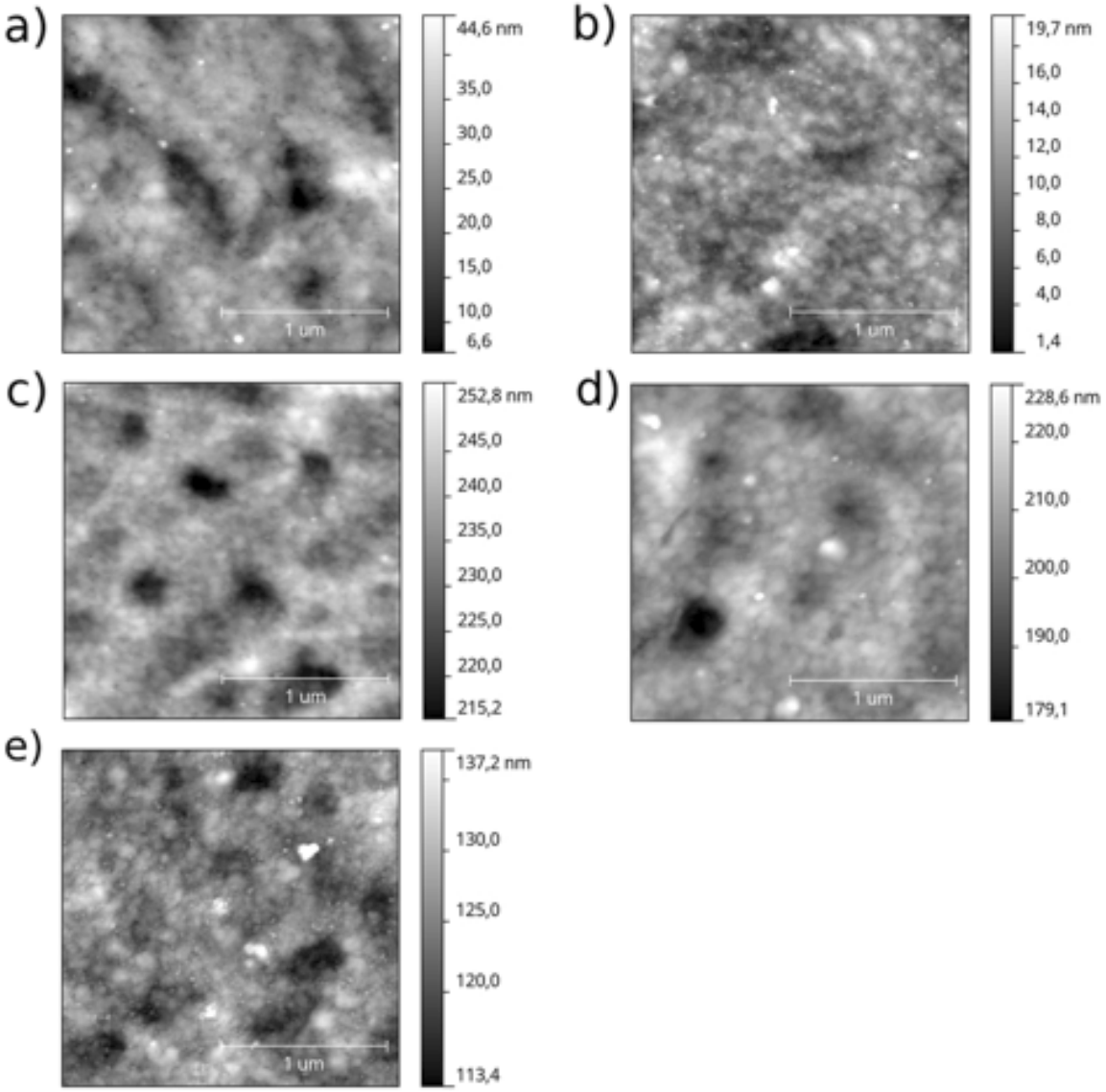

80

85